Smart Structures and Systems, Vol. 3, No. 4 (2007) 455-474

DOI: http://dx.doi.org/10.12989/sss.2007.3.4.455

Experimental verification of a distributed computing strategy for structural health monitoring

Y. Gao†

WSP Cantor Seinuk, 228 E. 45th St., New York, NY 10017, USA

B.F. Spencer, Jr.‡

Department of Civil and Environmental Engineering, University of Illinois at Urbana-Champaign, 205 N. Mathews Ave., Urbana, IL 61801, USA

(Received May 2, 2006, Accepted January 22, 2007)

Abstract. A flexibility-based distributed computing strategy (DCS) for structural health monitoring (SHM) has recently been proposed which is suitable for implementation on a network of densely distributed smart sensors. This approach uses a hierarchical strategy in which adjacent smart sensors are grouped together to form sensor communities. A flexibility-based damage detection method is employed to evaluate the condition of the local elements within the communities by utilizing only locally measured information. The damage detection results in these communities are then communicated with the surrounding communities and sent back to a central station. Structural health monitoring can be done without relying on central data acquisition and processing. The main purpose of this paper is to experimentally verify this flexibility-based DCS approach using wired sensors; such verification is essential prior to implementation on a smart sensor platform. The damage locating vector method that forms foundation of the DCS approach is briefly reviewed, followed by an overview of the DCS approach. This flexibility-based approach is then experimentally verified employing a 5.6 m long three-dimensional truss structure. To simulate damage in the structure, the original truss members are replaced by ones with a reduced cross section. Both single and multiple damage scenarios are studied. Experimental results show that the DCS approach can successfully detect the damage at local elements using only locally measured information.

Keywords: health monitoring; distributed computing; smart sensor; flexibility matrix; truss

1. Introduction

Structural health monitoring has attracted a significant amount of interest from researchers, with numerous SHM algorithms being developed, e.g., methods based on the measured frequency (Vandiver 1975, Cha and Tuck-lee 2000), flexibility-based methods (Pandey and Biswas 1994, 1995, Bernal 2002), parameter estimation methods (Yao, *et al*. 1992, Pothisiri and Hjelmstad 2003), neural network based methods (Kudva, *et al*. 1991, Kirkegaard, *et al*. 1995), etc. The vast majority of the existing methods require central acquisition and data processing, i.e., the measured data needs to be transferred

†Ph.D.
‡Newmark Endowed Chair, Professor, Corresponding Author, E-mail: bfs@uiuc.edu

to a central station, either through wired or wireless communication.

In the most general terms, damage can be defined as changes introduced into a system that adversely affects its performance (Farrar, *et al.* 1999). The effect of damage on structures can be classified as linear and nonlinear (Doebling, *et al.* 1996). Linear damage can be defined as the case when structures still behave linear-elastically after damage is introduced. In civil engineering structures, metal corrosion and concrete spalling/scour are typical damage events that may be defined as linear damage. Both corrosion and spalling/scour can significantly reduce the cross section of structural members, and therefore degrade the load capacity of the structure.

Damage in structures is an intrinsically local phenomenon. Responses from sensors close to the damaged site are expected to be more heavily affected than those remote to the damage. Trying to locate a few strategic sensors in structures such as the 2 km long Akashi-Kaikyo Bridge or the 443 m tall Sears Tower in Chicago so that these sensors can detect randomly occurring damage is intractable, if not impossible. To effectively detect arbitrary damage in structures, especially complicated structures, a dense array of sensors distributed over the entire structure will be required. However, if the measured data is to be centrally acquired, significant limitations will exist for conducting SHM either using wired or wireless sensors. Use of traditional wired sensors is difficult due to the cost of deploying and maintaining a large wiring plant. Similarly, transferring all the measured information to a central station using wireless senors is difficult because of power requirements and bandwidth limitations. In both cases, a tremendous amount of data is expected to be generated that would need to be sent to such a central station. Managing this large amount of data is challenging. Unnecessary information needs to be eliminated to efficiently utilize the network.

The recent development of the smart sensors has made health monitoring with a dense array of sensors feasible. A careful review of current smart sensing technology has been provided by Spencer, *et al.* (2002, 2004). The essential feature of a smart sensor is the on-board microprocessor, which grants these sensors their "smart" characteristic. A portion of the computation for damage detection can then be done at the sensor level. Extraneous information can be discarded, reducing the information that needs to be transferred back to the central station. The collection of large amounts of data for local and/or centralised processing to detect localized damage and its impact on global mode shapes could be enhanced, and the required networking and analytical effort reduced, by the spatial aggregation by local communities presented in this work.

Gao, *et al.* (2006) developed a new distributed computing strategy (DCS) which can take advantage of the distributed computing environment intrinsic to smart sensor technology. The main purpose of this paper is to experimentally verify this new DCS approach using wired sensors; such verification is essential prior to implementation on a smart sensor platform. In the sequel, the DLV method that forms the basis for the DCS approach is briefly reviewed. An overview of this flexibility-based DCS approach is then provided. Finally, experimental verification using a 5.6 m long three-dimensional truss structure is presented.

2. The damage locating vector method

Damage detection methods based on the flexibility matrix have recently been shown to be quite promising. In particular, Bernal (2002) proposed a flexibility-based damage localization method, the damage locating vector (DLV) method, which provides the foundation for the current work. The DLV method also has been experimentally verified in Gao, *et al.* (2004, 2007) and extended for continuous online monitoring employing ambient vibration in Gao and Spencer (2006). For completeness, the DLV method as employed herein is briefly reviewed in this section.

2.1. General concepts

The DLV method is based on determination of a special set of load vectors, the so-called damage locating vectors (DLVs). The DLVs have the property that when they are applied to the structure as static forces at the sensor locations, no stress is produced in the damaged elements. This unique characteristic can be employed to localize structural damage.

Assuming nominally linear structural behavior, the flexibility matrices at sensor locations are constructed from measured data before and after damage and denoted as $\mathbf{F}_u$ and $\mathbf{F}_d$, respectively. Then, all of the linear-independent load vectors $\mathbf{L}$ are collected which satisfy the following relationship.

$$\mathbf{F}_d\mathbf{L} = \mathbf{x} = \mathbf{F}_u\mathbf{L} \quad \text{or} \quad \mathbf{F}_\Delta\mathbf{L} = (\mathbf{F}_d - \mathbf{F}_u)\mathbf{L} = 0 \tag{1}$$

This equation implies that the load vectors $\mathbf{L}$ produce the same displacements $\mathbf{x}$ at the sensor locations before and after damage. From the definition, the DLVs are seen to also satisfy Eq. (1); that is, because the DLVs produce no stress in the damaged structural elements, the damage of those elements does not affect the displacements at the sensor locations. Therefore, the DLVs are indeed the vectors in $\mathbf{L}$.

To calculate $\mathbf{L}$, singular value decomposition (SVD) is employed. The SVD of the matrix $\mathbf{F}_\Delta$ leads to

$$\mathbf{F}_\Delta = \mathbf{U}\mathbf{S}\mathbf{V}^T = [\mathbf{U}_1 \ \mathbf{U}_0]\begin{bmatrix} \mathbf{S}_1 & 0 \\ 0 & 0 \end{bmatrix}[\mathbf{V}_1 \ \mathbf{V}_0]^T \tag{2}$$

$$[\mathbf{F}_\Delta\mathbf{V}_1 \mathbf{F}_\Delta\mathbf{V}_0] = [\mathbf{U}_1 \ \mathbf{S}_1 \ 0] \tag{3}$$

From Eq. (3), one obtains

$$\mathbf{F}_\Delta\mathbf{V}_0 = 0 \tag{4}$$

Eqs. (1) and (4) indicate that $\mathbf{L} = \mathbf{V}_0$, i.e., DLVs can be obtained from the SVD of the difference matrix $\mathbf{F}_\Delta$.

Each of the DLVs is then applied to an undamaged analytical model of the structure. The stress in each structural element is calculated and a normalized cumulative stress is obtained. The normalized cumulative stress for the jth element is defined as

$$\bar{\sigma}_j = \frac{\sigma_j}{\max\limits_k(\sigma_k)} \quad \text{where} \quad \sigma_j = \sum_{i=1}^{n} \text{abs}\left(\frac{\sigma_{ij}}{\max\limits_k(\sigma_{ik})}\right) \tag{5}$$

where σ_{ij} = stress in the jth element induced by the ith DLV; and σ_j = cumulative stress in the jth element. If an element has zero normalized cumulative stress $\bar{\sigma}_j$, then this element is a possible candidate of damage.

The DLV approach is a theoretically grounded procedure to interrogate changes in flexibility regarding the localization of stiffness related damage. In the absence of errors, the DLV approach offers the maximum resolution attainable from changes in flexibility (for a given sensor set). In this regard, it is worth noting that when the approach states that elements [a, b, c] are in the potentially damaged set the precise statement is that: “the complement of the set noted is not damaged”. In practice, due to truncation and many other approximations, however, the “potentially damaged set” is typically larger than the theoretical minimum because finite thresholds are necessary (Gao, *et al.* 2007).

2.2. Construction of flexibility matrix

As shown in the previous section, the flexibility matrices before and after damage need to be constructed to implement the DLV method. Note that Both $\mathbf{F}_u$ and $\mathbf{F}_d$ in Eq. (1) can be constructed from experimentally measured data so they are independent of an analytical model. Depending on whether or not the input excitations are measured, different formulations are needed to construct flexibility matrix from the measured data.

2.2.1. Forced vibration case

When the input is measured and there is at least one co-located sensor and actuator pair, Bernal and Gunes (2004) has shown how the experimental data can be used to obtain flexibility matrix for structures with general viscous damping. In their approach, the flexibility matrix is expressed as

$$\mathbf{F} = -\Psi\,\mathbf{D}_g\Psi^T \tag{6}$$

where Ψ = arbitrarily normalized complex mode shapes; $\mathbf{D}_g$ = diag($[d_1, d_2,\ldots, d_j,\ldots]$); and d_j = modal normalization constant that is obtained from

$$d_j = \lambda_j^{-(p+1)}\varphi_j^{-T}\mathbf{B}[\mathrm{diag}(\Psi_{m,j}^T\mathbf{q}_m)]^{-1} \tag{7}$$

where p = 0, 1, and 2 when measured outputs are displacement, velocity, and acceleration, respectively; λ and φ = eigenvalues and eigenvectors of state transition matrix $\mathbf{A}$ identified from measured data; φ_j^T = jth row of matrix φ^{-1}; $\Psi_{m,j}^T$ = jth row of matrix Ψ_m^T, with $\Psi_m = \mathbf{C}\varphi$, complex mode shapes at sensor locations; $\mathbf{B}$ = input influence matrix identified from measured data; and $\mathbf{q}_m$ = boolean matrix.

2.2.2. Ambient vibration case

For ambient vibration case, a mass perturbation method for construction of flexibility matrix suggested by Bernal (2004) can be used to construct the flexibility matrix for a linear structure with classical damping. Therein, the flexibility matrix takes the form

$$\mathbf{F} = (\psi\alpha)\Lambda^{-1}(\psi\alpha)^T \tag{8}$$

where ψ = undamped arbitrarily normalized mode shapes; Λ and ψ = solutions of the standard eigenproblem $\mathbf{K}\psi = \mathbf{M}\psi\Lambda$; α = diag($[\alpha_1, \alpha_2,\ldots, \alpha_j,\ldots]$); and α_j = modal normalization constant obtained from

$$\alpha_i^2 = \frac{\lambda_{0,i}-\lambda_{1,j}}{\lambda_{1,j}}\frac{q_{ij}}{\psi_{0,i}^T\Delta\mathbf{M}\,\psi_{1,j}} \tag{9}$$

where $\lambda_{0,i}$ and $\psi_{0,i}$ = ith eigenvalue and eigenvector of the original structure, respectively; $\lambda_{1,j}$ and $\psi_{1,j}$ = jth eigenvalue eigenvector of the modified structure, respectively; $\Delta\mathbf{M}$ = matrix describing the mass perturbation; and $\mathbf{q}_j = (\psi_0^T\psi_0)^{-1}\psi_0^T\psi_{1,j}$.

2.3. Extending the DLV method for continuous online SHM

The DLV method is not easily employed for continuous online damage diagnosis. For both forced and ambient vibration cases, a certain degree of interruption of structural operation will be needed to construct the flexibility matrix from measurements. The method based on forced vibration requires

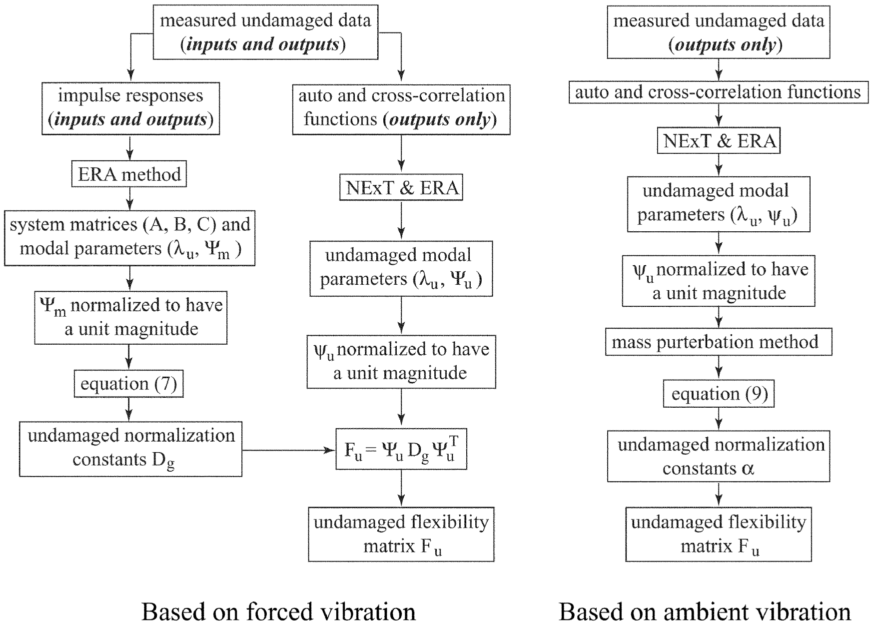

Fig. 1 Algorithm initialization

employing an external exciter, e.g., an impactor or a rotating imbalance vibrator, to shake the structure. The method based on ambient vibration requires adding mass to the structure to conduct dynamic testing. These methods can be used to construct the undamaged flexibility matrix. However, computing the damaged one by one of these methods each time the health of the structure is assessed is intractable.

Gao and Spencer (2006) proposed an algorithm which extends the DLV method for continuous online monitoring. The essence of the approach is to construct an approximate flexibility matrix for the damaged structure utilizing the undamaged normalization constants with the mode shapes before and after damage being normalized to have a unit magnitude.

The first step of the proposed algorithm is to compute the undamaged normalization constants and then the undamaged flexibility matrix from the measured data. This step is termed algorithm initialization. Once the initialization is completed, the second step of the proposed approach is to construct an approximate flexibility matrix for the potentially damaged structure employing ambient vibration and then to apply the DLV method to detect damage in the structure. Herein, this step is referred as algorithm operation. The flow charts for the algorithm initialization and operation are shown in Figs. 1 and 2. This extended DLV method is incorporated into the proposed DCS approach, which is presented in section 3.

For more detailed information regarding the DLV method, the interested reader is directed to Bernal (2002), Gao and Spencer (2006), and Gao, *et al*. (2007).

3. Distributed computing strategy (DCS)

3.1. Hierarchical organization

The conceptual hierarchical organization of the DCS approach is shown in Fig. 3. Different hierarchical organizations have been proposed by researchers for different applications in recent years (Frampton

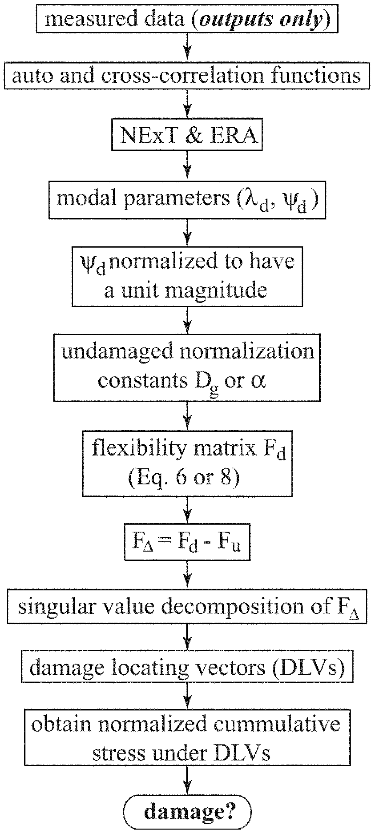

Fig. 2 Algorithm operation

2001, Akyildiz, *et al.* 2002, Lynch 2002). In contrast to traditional SHM algorithms which require all the measured information to be transferred to a central station, the measured information is aggregated locally by a selected sensor within the sensor group, termed the manager sensor, and only limited information is sent back to the central station to provide the condition of the structure. Small numbers of smart sensors are grouped to form different communities. For clarity, this figure shows each sensor as being included in only one community; however, in the proposed approach, each sensor can participate in multiple communities. For each community, the manager sensor collects measured responses and implements the damage detection algorithm for this community. Adjacent manager sensors need to interact with each other to exchange damage information. Referring again to Fig. 3, manager sensors in communities 1, 2, and 3 interact with each other while community 4 only interacts with community 3.

After the measured information is aggregated locally, the manager sensor determines what information needs to be sent back to the central station. In the proposed approach, each of the communities in which damage has not occurred only transmits an “ok” signal to the central station, which is reflected by the dotted line connection in Fig. 3. The communities in which damage has occurred need to send information about the damaged elements, which is reflected by the solid line connection in Fig. 3. In this way, only limited information needs to be transferred between sensors throughout the entire

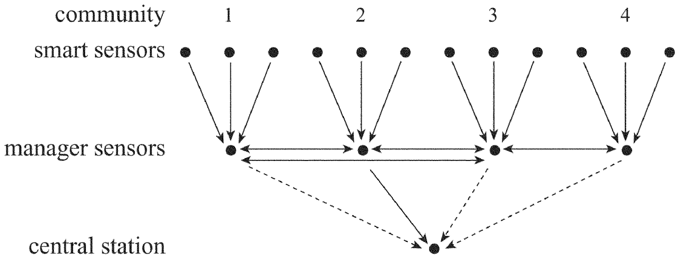

Fig. 3 Sketch of hierarchical organization

structure. This approach will significantly reduce the communication traffic and the associated power demands in the sensor network.

3.2. Strategy implementation

The planar truss structure shown in Fig. 4 is employed to illustrate the details of the implementation of the proposed SHM strategy. In this truss, structural nodes are numbered starting from left to the right, with all the odd numbers at the lower chord, and all the even numbers at the upper chord except node 28 which is at the right support. Each structural node number has a circle around it.

3.2.1. Community development

First, the sensor communities are formed. A single community includes a set of adjacent structural nodes, sensors on these nodes, and members. These structural members have both ends connected to the structural nodes in the same community. Fig. 4 shows an example of how communities can be formed. Sensors on every three consecutive lower chord nodes and the corresponding upper chord nodes are grouped together to monitor those elements connected to these nodes. A total of 11 different localized sensor groups are formed from left to right in this truss structure. As an example, community 6 in Fig. 4 includes nodes [12 13 14 15 16 17] and elements [23 24 25 26 27 28 29 30 31]. Only the elements which have both ends connected to community nodes are monitored by the manager sensor for this community.

To allow for some computational redundancy, adjacent communities are recommended to have some overlaps so that each structural member is monitored by more than a single community.

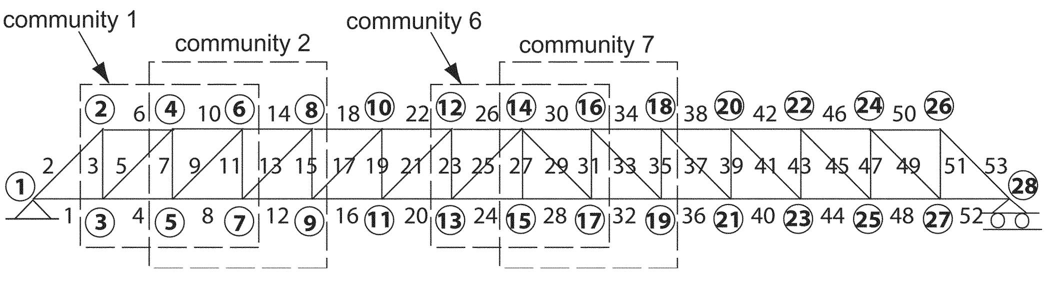

Fig. 4 14-bay truss structure

3.2.2. Computing undamaged normalization constants for communities

Once the community is formed, the modal normalization constants for the undamaged structure have to be computed to construct the flexibility matrix employing either forced or ambient vibration. For this purpose, one sensor from each community, termed the reference sensor, will be required to send the recording data to the central station. These reference sensors are selected such that their mode shape magnitudes will not be zero for the modes of interest. The modal parameters associated with these reference sensors, denoted as $\hat{\Psi}_j$ or $\bar{\lambda}_j$ and $\hat{\psi}_j$ respectively, are identified using the Eigensystem Realization Algorithm (ERA) (Juang and Pappa 1985) or the Natural Excitation Technique (NExT) (James, *et al.* 1993) in conjunction with the ERA method. The undamaged normalization constants can then be computed based on the methods presented in section 2.2, and denoted as $\hat{d}_j$ or $\hat{\alpha}_j$.

After the undamaged normalization constants are obtained, the SHM system can start measuring data to construct the undamaged and damaged flexibility matrices for use in continuous online monitoring employing only ambient vibration.

However, the normalization constants $\hat{d}_j$ or $\hat{\alpha}_j$ can't be employed directly by each community for damage detection, because the scalar for the jth mode shape $\hat{\Psi}_j$ or $\hat{\psi}_j$ and the jth mode shape Ψ_j^i or ψ_j^i in ith community can be different. The jth undamaged normalization constant for the ith community d_j^i or α_j^i can be obtained as

$$d_j^i = \hat{d}_j \cdot \left(\frac{\hat{\Psi}_j(i)}{\hat{\Psi}_j^i(k)}\right)^2 \quad \text{and} \quad \alpha_j^i = \hat{\alpha}_j \cdot \left(\frac{\hat{\psi}_j(i)}{\hat{\psi}_j^i(k)}\right) \tag{10}$$

where j = jth mode; i = ith community; and k = reference sensor location in the ith community. The undamaged normalization constants for the ith community are $\mathbf{D}_g^i = [d_1^i, d_2^i, \ldots d_j^i]$ or $\alpha^i = [\alpha_1^i, \alpha_2^i, \ldots \alpha_j^i]$.

3.2.3. Data aggregation - detecting damage

To minimize the communication traffic in the sensor network, measured data need to be transferred to the manager sensor for data processing.

Clocks of smart sensors in the same community are first synchronized with each other. The measurements are then collected, which will need to be transferred to the manager sensor for computation. To facilitate communication, the manager sensor should be centrally located to the other sensors in the community. For example, in Fig. 5, the sensors at structural node 15 is selected as the manager sensor for community 6. As can be seen from the figure, some sensors may need to transfer information to more than one manager sensors. This situation occurs when the smart sensors participate in different communities.

After the data have been transferred to the manager sensor, computation can be conducted using the on-board microprocessor to locate the damage within the community. The extended DLV method

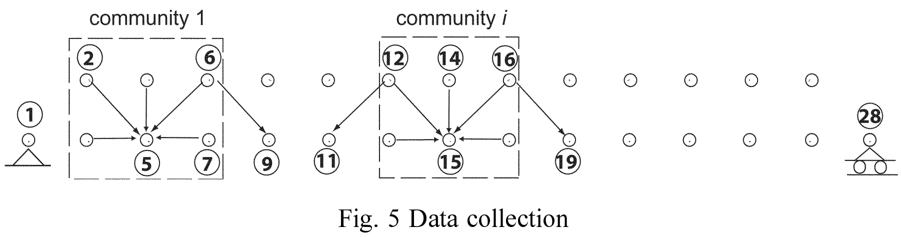

Fig. 5 Data collection

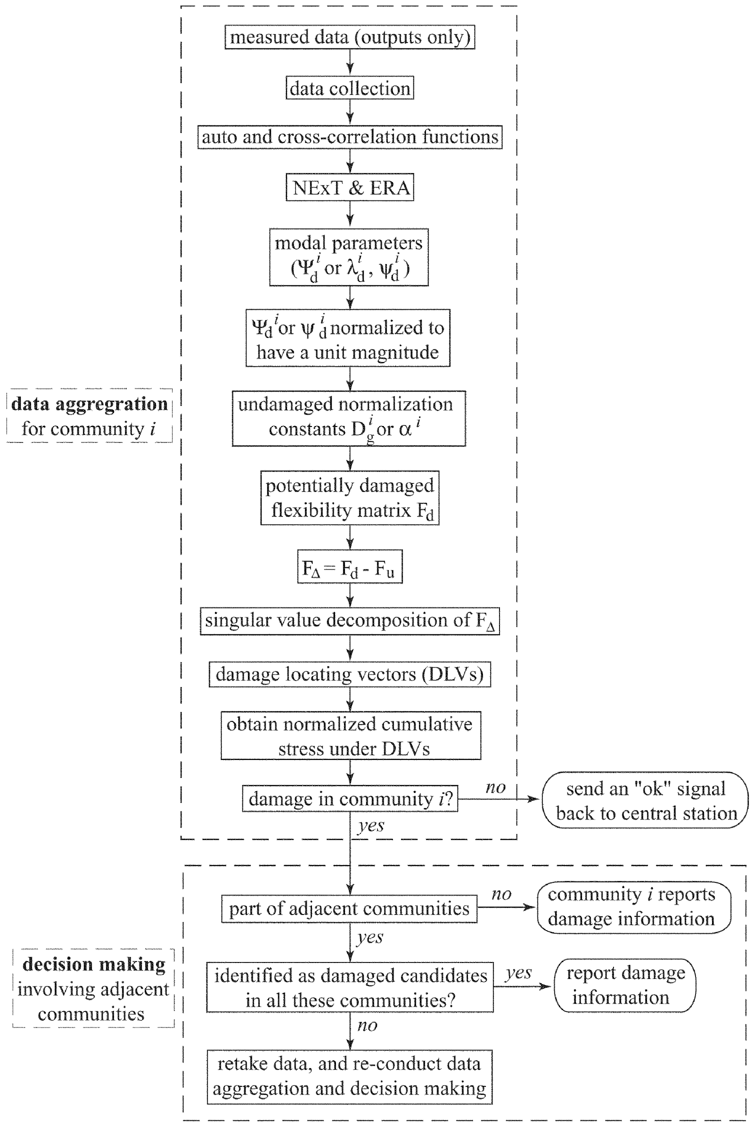

Fig. 6 Data aggregation and decision making

presented in section 2.3 is incorporated in this SHM strategy to localize the damage in each community. The flow chart for damage aggregation in a community is shown in Fig. 6.

3.2.4. Decision making

Actions need to be taken after the data aggregation is done for a community. If there is no damage detected in a community, the manager sensor does not initiate interaction with other manager sensors; rather, it simply sends an “ok” signal back to the central station. If there is damage identified in a community, the manager sensor needs to send queries to its counterpart in adjacent communities. There are three possibilities after sending the queries:

- The damage candidate in community *i* does not participate in adjacent communities. The manager sensor in community *i* sends the damage information back to the central station.
- The damage candidate in community *i* participates in other communities and identified as the potentially damaged location in all of these communities. This damage candidate is then confirmed and reported to the central station by these communities.
- The damage candidate identified by community *i* participates in other communities, but not all of the communities identify it as the potentially damaged element. These communities then need to retake data and re-conduct data aggregation and decision making.

A flow chart for the decision making is shown in Fig. 6.

4. Experimental verification

4.1. Experimental setup

The DCS strategy is experimentally verified using a three-dimensional truss structure (see Fig. 7). This structure was tested at the Smart Structures Technology Laboratory (SSTL) of the University of Illinois at Urbana-Champaign (*http://cee.uiuc.edu/sstl/*). The length of each bay of the truss is 0.4 m on each side. The truss sits on two rigid supports. One end of the truss is pinned to the support, and the other is roller-supported. The pinned end can rotate freely with all three translations restricted. The roller end can move in the longitudinal direction. The total mass of the truss structure is about 90 kg (not including the two end rigid supports) and the first natural frequency is about 20 Hz.

The truss members are steel tubes with an inner diameter of 1.09 cm and an outer diameter of 1.55 cm. The joints of the elements are specially designed so that the truss member can be easily removed or replaced to simulate damage without dissembling the entire structure. A detailed picture of the joint is shown in Fig. 7. As can be seen, the truss member can be removed by unscrewing the collars at the both ends of the member toward the joint. On the other hand, if the collar is screwed away from the joint, this member can be easily installed.

A Ling Dynamic Systems permanent magnetic V408 shaker is attached to the bottom nodes of this panel to excite the structure vertically. A load cell with a sensitivity of 89 N/volt is installed between the shaker and the bottom of the joint to monitor and measure the input to the structure (see Fig. 8).

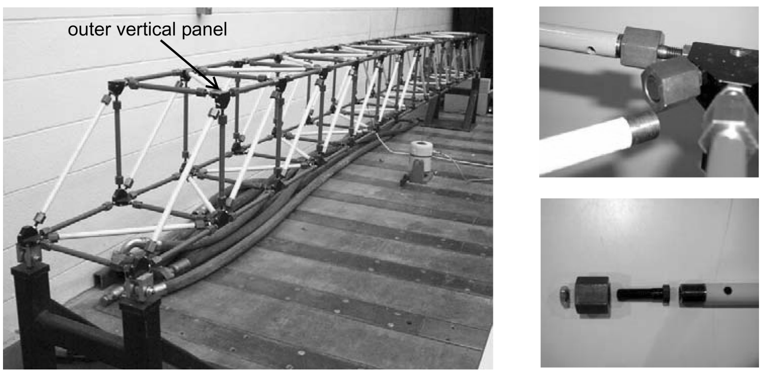

Fig. 7 5.6 m long truss structure

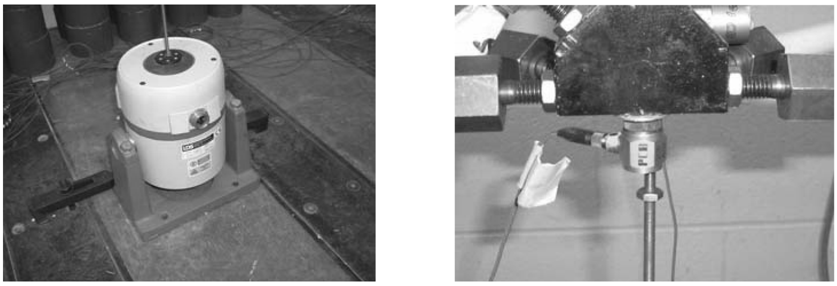

Fig. 8 Magnetic shaker and load cell

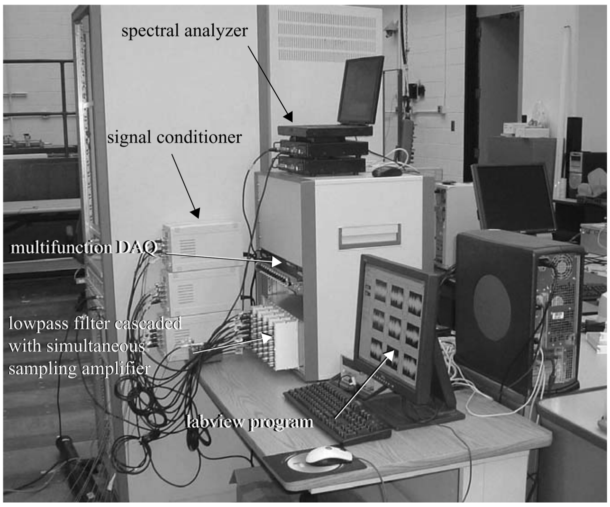

Fig. 9 Experimental setup

The dynamic testing system shown in Fig. 9 has been developed to support this experiment. The magnetic shaker and the truss structure are not in the picture. There is a data acquisition system from National Instruments. The key components for this data acquisition system are the data acquisition (DAQ) board NI PCI-6052E, the lowpass elliptical filter NI SCXI-1141, and the simultaneous-sampling differential amplifier NI SCXI-1140.

The National Instruments SCXI-1141 is an 8-channel, programmable 8th-order lowpass elliptical filter, which allows a sharp roll off of the response. By passing the measured data through this lowpass filter, the component of the signal at frequencies higher than the cut-off frequency will be significantly reduced. The cut-off frequency of this filter is user selectable in the range from 10 Hz to 25 KHz.

The National Instruments SCXI-1140 is an 8-channel simultaneous sample and hold differential amplifier module. Simultaneous sampling is very important for dynamic testing with multiple channel measurements, because any differences in the sample times will result in artificial phase lags in the data. With the SCXI-1140, sampling of multiple signals can be achieved with negligible phase delay between channels. The SCXI-1140 is cascaded with the SCXI-1141 for applications requiring filtering and simultaneous sampling to provide high quality dynamic measurements.

A Labview program has been developed to acquire and save the data from this National Instruments data acquisition system. This program allows the programmable cut-off frequencies to be set for the lowpass filter, the gain on each measurement channel to be adjusted, the sampling rate and measuring time to be specified, etc. The cut-off frequency is set to be 100 Hz, resulting in a the sampling rate of 256 Hz for this experiment.

Ideally, all the structural members should be monitored for damage. Due to limited experimental equipment, only elements in the outer vertical panel of the truss are monitored employing the proposed DCS approach. A sketch of this panel is depicted in Fig. 4 with each node number having a circle around it.

Sensor communities are formed as shown in Fig. 4. There are a total of 12 accelerometers in a sensor community with one accelerometer in the vertical direction and the other in longitudinal direction at each structural node. Accelerations are measured directly from these PCB high sensitivity piezotronics accelerometers (model 353B33). When implemented on smart sensors (e.g. Intel's Imote2), MEMS-based sensors will likely be used. These localized sensors are used to monitor the condition of nine local structural members which have both ends connected to the structural nodes in the same community. Again, there are a total of 11 sensor communities in this experiment.

One of the communities with a single member replaced by the damaged one is displayed in Fig. 10. Due to the limited experimental equipment, while the measurements in the same community are made simultaneously, these 12 accelerometers shown have to be moved along the truss structure to measure the responses for each community.

4.2. Algorithm initialization

To detect the damage in this truss structure employing the proposed DCS approach, the undamaged flexibility matrix at the sensor communities needs to be constructed. Construction of the flexibility matrix based on both forced and ambient vibration employing experimental data is investigated.

For the case of initialization based on forced vibration, dynamic testing is conducted when seven accelerometers are installed at nodes [7, 11, 13, 17, 19, 21, 23] to measure the acceleration in the vertical direction and the shaker is attached to the bottom of node 17. Therefore, there is one co-located sensor and actuator pair which is at node 17. Modal normalization constants associated with these mode shapes can then be obtained from experimental data using Eq. (7).

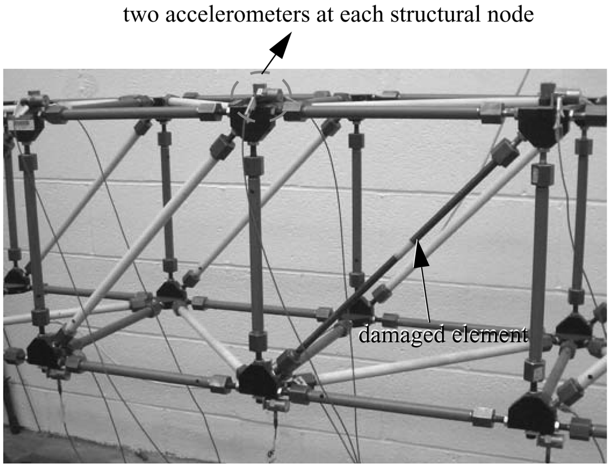

Fig. 10 Example of a single sensor community for the outer vertical panel of the truss

For the case of algorithm initialization based on ambient vibration, accelerometers were installed at the vertical direction of nodes [7, 9, 11, 13, 15, 17, 19, 21, 23, 25] and at the longitudinal and transverse direction of node 11. A lumped mass of 1.124 kg, which is about 48% of the original nodal mass, was attached to the bottom of node 11 to simulate mass perturbation. The modal normalization constants can be obtained based on the mass perturbation method using Eq. (9).

To verify the results from both of these approaches, undamaged flexibility matrices for the vertical direction of nodes [7, 11, 13, 17, 19, 21, 23] have been computed using Eqs. (6) and (8) employing the first six dominant modes. Good agreement has been shown in Tables 1 and 2.

After the modal normalization constants associated with the mode shapes at reference sensor locations were determined, a series of dynamic testing was conducted with 12 sensors installed in each community to obtain the mode shapes in these communities under ambient vibration. The associated modal normalization constants in each of these communities can then be obtained from Eq. (10) and the undamaged flexibility matrix at each community can be constructed using Eqs. (6) and (8).

Based on the contribution of the modes to the measurements, different communities might need to utilize different modes to construct the flexibility matrix. Fig. 11 shows a total of 12 cross spectral density functions for communities 4 and 8, respectively. These cross spectral density functions are computed from the measurements of the 12 accelerometers in one community, with the vertical acceleration at node 9 being selected as the reference output for community 4, and the vertical acceleration at node 21 being selected as the reference output for community 8. The first 5 dominant modes are identified for both communities 4 and 8. As shown in Fig. 11, the fourth dominant mode is different for these two communities.

In this experimental validation, flexibility matrices in communities 1 through 5 are constructed using the same dominant modes as community 4, and communities 6 through 11 use the same dominant modes

Table 1 Undamaged flexibility matrices based on forced vibration ($\times 10^{-5}$ m/N)

Normalization constants based on forced vibration						
0.0533	0.0704	0.0703	0.0604	0.0533	0.0414	0.0321
0.0704	0.0958	0.0977	0.0885	0.0809	0.0651	0.0526
0.0703	0.0977	0.1012	0.0949	0.0887	0.0732	0.0604
0.0604	0.0885	0.0949	0.0960	0.0936	0.0804	0.0689
0.0533	0.0809	0.0887	0.0936	0.0935	0.0819	0.0714
0.0414	0.0651	0.0732	0.0804	0.0819	0.0730	0.0646
0.0321	0.0526	0.0604	0.0689	0.0714	0.0646	0.0579

Table 2 Undamaged flexibility matrices based on ambient vibration ($\times 10^{-5}$ m/N)

Normalization constants based on ambient vibration						
0.0539	0.0695	0.0690	0.0568	0.0489	0.0375	0.0286
0.0695	0.0930	0.0951	0.0838	0.0756	0.0609	0.0488
0.0690	0.0951	0.0993	0.0917	0.0850	0.0705	0.0579
0.0568	0.0838	0.0917	0.0930	0.0906	0.0788	0.0674
0.0489	0.0756	0.0850	0.0906	0.0906	0.0805	0.0700
0.0375	0.0609	0.0705	0.0788	0.0805	0.0728	0.0642
0.0286	0.0488	0.0579	0.0674	0.0700	0.0642	0.0572

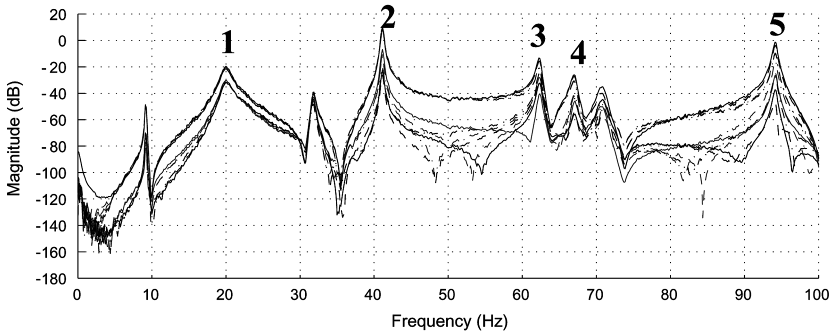

Community 4

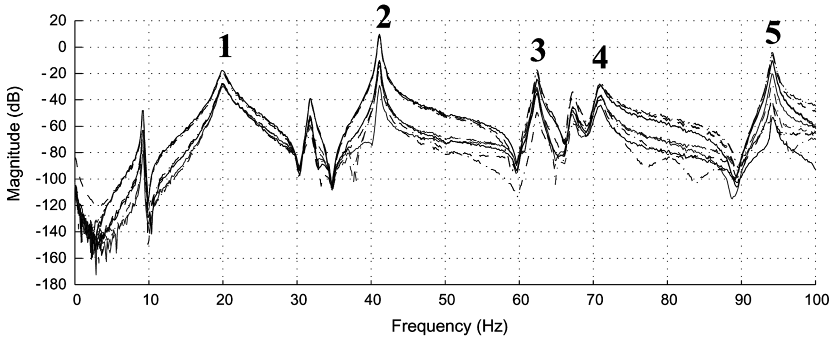

Community 8

Fig. 11 Cross spectral density functions

as community 8. Therefore, the flexibility matrix in each community is constructed using the first five dominant modes determined from the measurements.

4.3. Damage detection and decision making

Once algorithm initialization is finished, the sensors can start collecting data from the structure to monitor its condition.

A series of damage detection tests have been conducted using the 14-bay three-dimensional truss structure located at SSTL of UIUC. Structural damage is simulated by replacing an original elements with ones having a 52.7% cross section reduction, which results in a small axial stiffness reduction in different members (see Table 3).

Three excitation conditions (see Table 4) have been investigated. As shown in the table, excitation condition 1 has the same excitation location, magnitude, and bandwidth before and after damage. Under this excitation condition, the shaker is attached to the bottom of node 17 to excite the structure vertically.

Table 3 Structural damage

	Longitudinal element	Vertical element	Diagonal element
Cross section reduction	52.7%	52.7%	52.7%
Equivalent axial stiffness reduction	44%	43.5%	46.9%

Table 4 Various excitation conditions before and after damage

	Location	Magnitude	Bandwidth
Condition 1	same	same	same
Condition 2	same	different	different
Condition 3	different	different	different

Table 5 Damage cases

Cases	Excitation condition	Damaged elements
Case 1	condition 1	vertical element 7 and longitudinal element 36
Case 2	condition 2	longitudinal element 8
Case 3	condition 3	diagonal element 9

A band-limited white noise with a 0.1 RMS voltage and a bandwidth of 100 Hz is sent from the Siglab spectral analyzer to drive the shaker.

To better simulate the ambient vibration conditions in which the excitation contents can be changed, performance of the proposed approach under excitation conditions 2 and 3 is also studied. Under condition 2, the magnitude of the band-limited white noise excitation is changed from a RMS voltage of 0.1 to 0.08, and the bandwidth is changed from 100 Hz to 200 Hz before and after damage. For condition 3, not only are the excitation bandwidth and magnitude different, the shaker is also relocated from node 17 to node 23 before and after damage.

Results from three damage cases (see Table 5) are presented in the remainder of the paper. The process of retaking data when there is inconsistent damage information is not investigated in case 1. Instead it will be studied in cases 2 and 3.

A cut-off value of 0.3 for the normalized cumulative stress is used and provides good performance for a wide range of damage cases by using a total of five DLVs associated with the smallest singular values. This cut-off value will be used to select the damaged elements from the detection results.

4.3.1. Case 1

The detection results regarding damage in vertical element 7 and longitudinal element 36 are shown in Fig. 12. The damaged elements have been correctly identified for both cases of initialization based on forced and ambient vibration.

For the case of initialization based on ambient vibration, community 2 identifies element 9 as possibly having damage because its normalized cumulative stress is smaller than the threshold value of 0.3. However, community 1 reports this element as undamaged because its stress is larger than the threshold. Inconsistent information regarding the condition of element 9 is obtained in community 1 and 2; therefore, these communities need to retake data and re-conduct damage detection. Similarly, communities 9 and 10 need to retake data and re-conduct damage detection regarding element 40. As mentioned previously, the process of re-conducting damage detection is not investigated in this case.

4.3.2. Case 2

Damage detection results when longitudinal element 8 is damaged are shown in Fig. 13. Element 8 is successfully identified as the damage candidate in both cases as its computed normalized cumulative stress is smaller than the threshold.

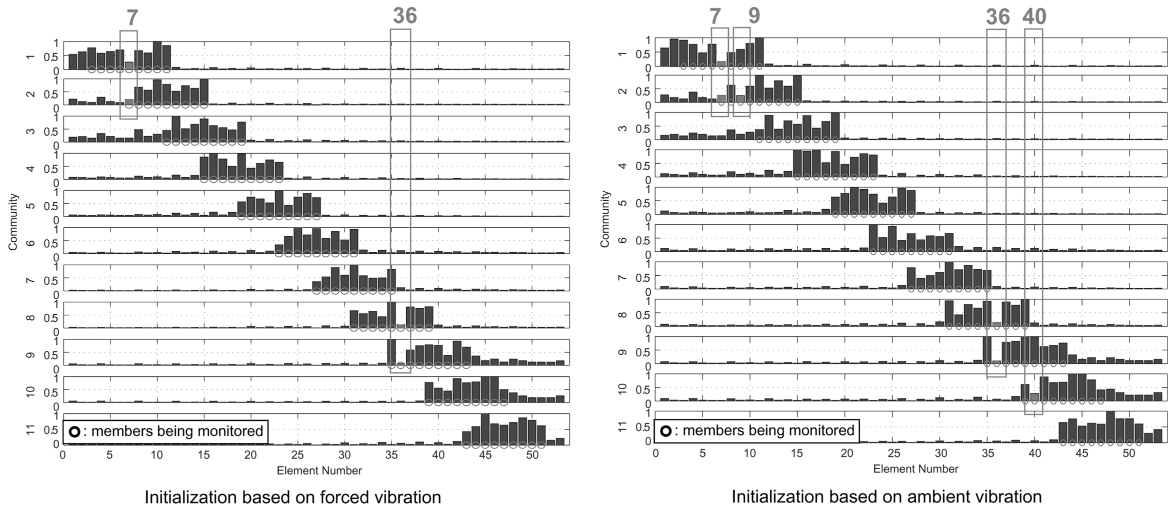

Fig. 12 Normalized cumulative stress when elements 7 and 36 are damaged

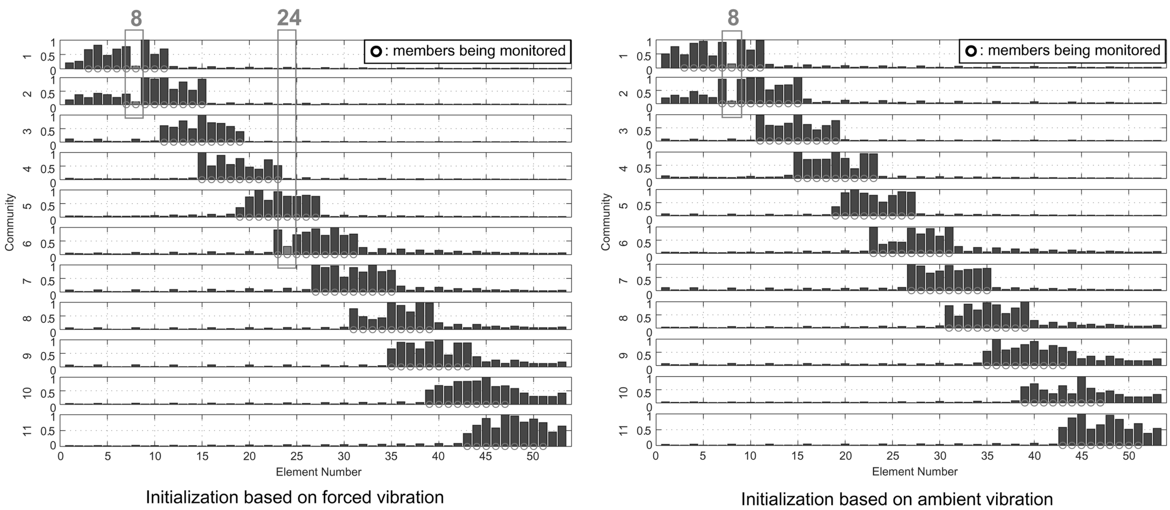

Fig. 13 Normalized cumulative stress when element 8 is damaged

For the case of initialization based on forced vibration, community 6 reports that element 24 is damaged as it has a normalized cumulative stress smaller than the threshold value of 0.3. However, community 5 identify element 24 as having no damage as its stress exceeds the threshold. Inconsistent information is obtained by communities 5 and 6 regarding the condition of element 24, therefore these two communities need to retake data and re-conduct damage detection to determine its condition. Fig. 14 shows the results after re-conducting damage detection in these two communities; element 24 is determined as undamaged because both communities report that it has a normalized cumulative stress larger than the threshold. Therefore, only communities 1 and 2 report damage information to the central station, while other communities send “ok” signal back to the central station.

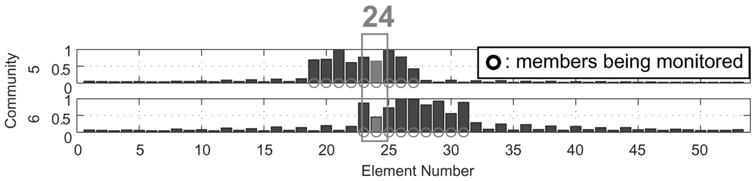

Fig. 14 Normalized cumulative stress when element 8 is damaged (retaking data regarding element 24 in communities 5 and 6)

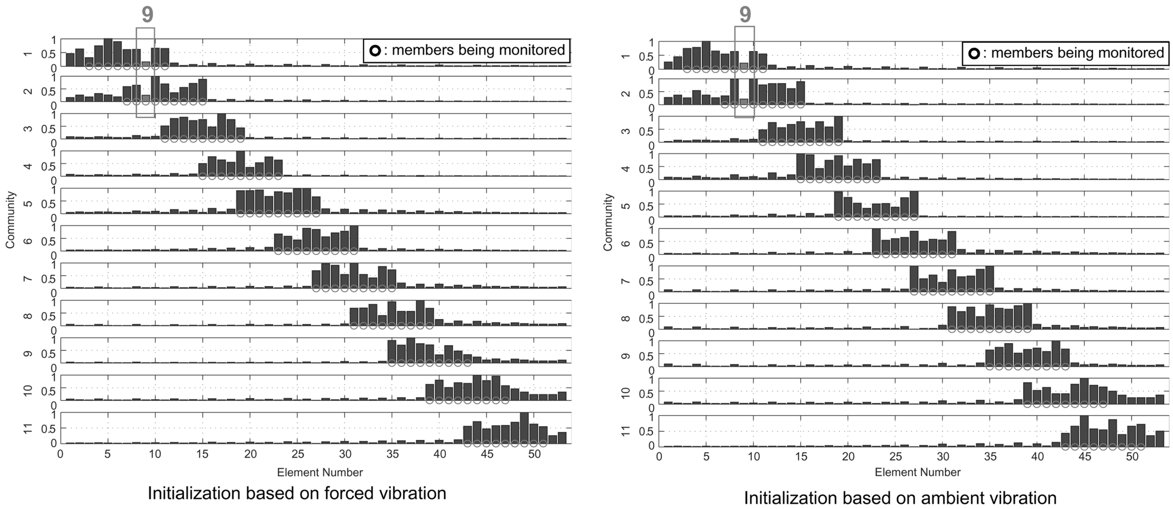

Fig. 15 Normalized cumulative stress when element 9 is damaged

4.3.3. Case 3

Fig. 15 shows the damage detection results when element 9 is damaged. In both cases, element 9 is consistently identified as the damage candidate; and there is no other damage. Therefore, only communities 1 and 2 report the damage information and other communities only need to send a "ok" signal back to the central station.

These experimental results demonstrate that the proposed DCS approach not only works robustly when the excitation remains the same before and after damage, but also performs well when excitation contents have been changed. Therefore, the proposed approach is promising for applications requiring a dense array of smart sensors.

5. Discussions

In this experiment, inconsistent damage information is obtained in various damage cases. Questions arise regarding how frequently this situation happens, as well as how reliable the proposed algorithms can detect structural damage. This section provides some insights into these questions and discusses limitations and challenges faced for full-scale implementation of the proposed DCS approach.

To investigate the situation of inconsistent damage information, case 2 in which element 8 is damaged is further considered. As shown in Fig. 13, for the case of initialization from forced vibration, inconsistent

Table 6 Excitation conditions for ten sequential experiments: element 8 is damaged

Tests		Excitation bandwidth (Hz)	Excitation magnitude (RMS value)
Undamaged		100	0.10
Damaged	Test 1	200	0.06
	Test 2	200	0.08
	Test 3	200	0.10
	Test 4	200	0.12
	Test 5	200	0.14
	Test 6	100	0.06
	Test 7	100	0.08
	Test 8	100	0.10
	Test 9	100	0.12
	Test 10	100	0.14

information regarding element 24 is obtained by community 6. For this specific community, a total of ten sequential tests were conducted for the damaged structure. The excitation conditions for these ten tests are listed in Table 6. The damage detection results from community 6 are shown in Fig. 16. As can be seen, among these ten tests, only tests 1 and 7 reports false positive results, and then not for the same element. Although these results are problem dependent, they indicate that the situation of inconsistent damage information is rather random and does not occur in the majority of the tests.

To provide insight into how reliable the proposed DCS approach can detect the damage, case 2 is considered again. Ten sequential tests are conducted for community 2 with the excitation conditions as shown in Table 6. The damage detection results are displayed in Fig. 16, which shows element 8 is identified as the damage candidate. These results indicate the proposed DCS approach can consistently identify the damage location, in this case, element 8.

The truss structure tested in this experiment is used to illustrate the DCS method, but should not be taken to imply that the proposed DCS approach is only for a specific type of structure, i.e., bridges. Similar to other damage detection methods that require information from the undamaged structure for the purpose of comparison, a dynamic test (forced or ambient vibration test) is needed to establish such a baseline model. After that, the DCS approach can be implemented to monitor the structure based only on output response information, therefore interruption of the operation of the structure can be avoided.

The proposed DCS approach only addresses the case of linear damage in structures, which means the measured response before and after damage should be linear. The method developed here is expected to be able to accommodate various cases of linear damages that result in a loss of structural stiffness. However, if the structure's damage does not cause any change of the identified modal properties (modal frequency and mode shape), this type of damage cannot be detected by the proposed DCS approach.

While the DCS approach has shown significant promise for application of SHM on a densely distributed sensor network, implementation on smart sensors and full-scale validation studies are still needed.

6. Conclusions

In this paper, a flexibility-based distributed computing strategy for SHM was experimentally verified using a 6.5 m long three-dimensional truss structure. The damage locating vector method that forms the

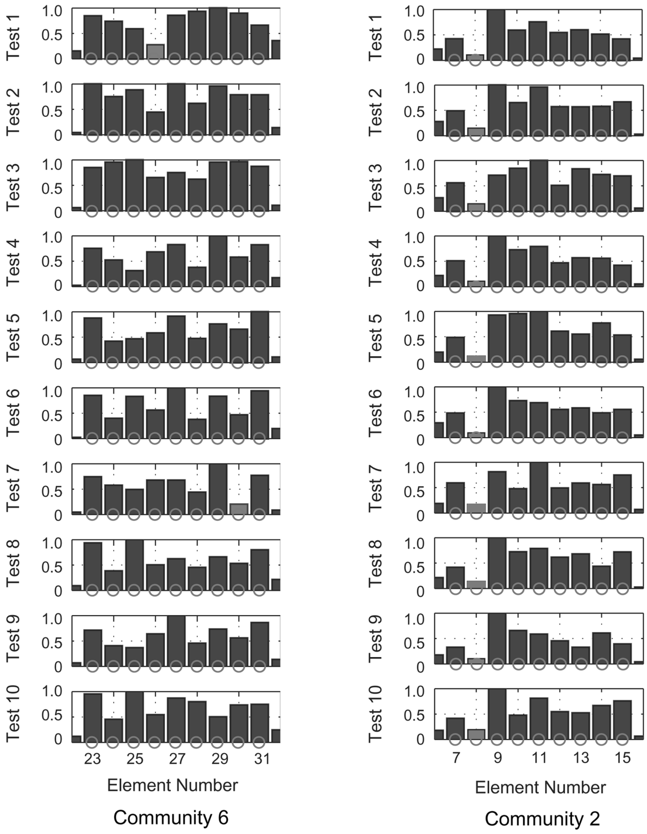

Fig. 16 Normalized cumulative stress when element 8 is damaged

basis of the DCS approach was reviewed. An overview of the distributed computing strategy was then presented. A description of the experimental setup was provided, followed by the detailed description and discussions of the experimental results. Structural damage was simulated by replacing various truss elements with ones having a 52.7% cross section reduction. Both single and multiple damage scenarios were studied. Various excitation conditions, including changing excitation level, bandwidth and location before and after damage, were also investigated. Retaking data and re-conducting damage detection when there is inconsistent damage information were studied using experimental data.

The experimental results have shown that the proposed DCS approach can successfully monitor local community members utilizing only locally measured information for various damage scenarios under different excitation conditions. Situation of inconsistent damage information was shown rather random and did not occur in the majority of the tests. The proposed DCS approach was shown promising for application of SHM on a densely distributed sensor network. Implementation of the DCS on Intel's Imote2 Smart sensor platform is currently underway.

Acknowledgements

The authors gratefully acknowledge the support of the research by the National Science Foundation under NSF grants CMS 03-01140 and CMS 06-00433, Dr. S.C. Liu, Program Director.

References

Akyildiz, I. F., Su, W., Sankarasubramaniam, Y. and Cayirci, E. (2002), "Wireless sensor networks: a survey", *Computer Networks*, **38**, 393-422.

Bernal, D. (2002), "Load vectors for damage Localization", *J. Eng. Mech.*, **128**(1), 7-14.

Bernal, D. and Gunes, B. (2004), "Flexibility based approach for damage characterization: benchmark application", *J. Eng. Mech.*, **130**(1), 61-70.

Bernal, D. (2004), "Modal scaling from known mass perturbations", *J. Eng. Mech.*, **130**(9), 1083-1088.

Cha, P. D. and Tuck-Lee, J. P. (2000), "Updating structural system parameters using frequency response data", *J. Eng. Mech.*, **126**(12), 1240-1246.

Doebling, S. W., Farrar, C. R., Prime, M. B. and Shevitz, D. W. (1996), "Damage identification and health monitoring of structural and mechanical systems from changes in their vibration characteristics: a literature review", Los Alamos National Laboratory Report LA-13070-MS.

Farrar, C. R., Doebling, S. W. and Duffey, T. A. (1999), "Vibration-based damage detection", *Proc. of the Structural Dynamics Forum SD2000*, Los Alamos, NM, 11-17.

Frampton, K. D. (2001), "Decentralized control of structural acoustic radiation", *Proc. of International Mechanical Engineering Congress and Exhibition*, New York, NY, **28**, 232-238.

Gao, Y. and Spencer, Jr., B. F. (2006), "Online damage diagnosis of civil infrastructure employing a flexibility-based approach", *J. Smart Mater. Struct.*, **15**, 9-19.

Gao, Y. Spencer, Jr., B. F. and Bernal, D. (2004), "Experimental verification of the damage locating vector method", *Proc. of the 1st International Workshop on Advanced Smart Materials and Smart Structures Technology*, Honolulu, Hawaii.

Gao, Y. Spencer, Jr., B. F. and Bernal, D. (2007), "Experimental verification of the flexibility-based damage locating vector method", *J. Eng. Mech.*, accepted.

Gao, Y., Spencer, B. F., Jr. and Ruiz-Sandoval, M. (2006), "Distributed computing algorithm for structural health monitoring", *J. Struct. Control Health Monit.*, **13**(1), 488-507.

James, G. H. III, Carne, T. G. and Lauffer, J. P. (1993), "The Natural Excitation Technique (NExT) for modal parameter extraction from operating wind turbines", SAND92-1666, UC-261, Sandia National Laboratories.

Juang, J. N. and Pappa, R. S. (1985), "An eigensystem realization algorithm for modal parameter identification and model reduction", *J. Guidance Control Dyn.*, **8**, 620-627.

Kirkegaard, P., Nielsen, S. and Hansen, H. (1995), "Identification of nonlinear structures using recurrent neural networks", *Proc. of the 13th International Modal Analysis Conf.*, pp. 1128-1134.

Kudva, J., Munir, N. and Tan, P. (1991), "Damage detection in smart structures using neural networks and finite element analysis", *Proc. of ADPA/AIAA/ASME/SPIE Conf. on Active Materials and Adaptive Structures*, pp. 559-562.

Lynch, J. P. (2002), "Decentralization of wireless monitoring and control technologies for smart civil structures", PhD thesis, Stanford University, CA.

Pandey, A. K. and Biswas, M. (1994), "Damage detection in structures using changes in flexibility", *J. Sound Vib.*, **169**(1), 3-17.

Pandey, A. K. and Biswas, M. (1995), "Damage diagnosis of truss structures by estimation of flexibility change", *The Int. J. Analytical and Experimental Modal Analysis*, **10**(2), 104-117.

Pothisiri, T. and Hjelmstad, K. D. (2003), "Structural damage detection and assessment from modal response", *J. Eng. Mech.*, **129**(2), 135-145.

Spencer, Jr., B. F., Ruiz-Sandoval, M. and Gao, Y. (2002), "Frontiers in structural health monitoring", *Proc. of China-Japan Workshop on Vibration Control and Health Monitoring of Structures and Third Chinese Symposium on Structural Vibration Control*, Shanghai, China, December 8-12.

Spencer, Jr., B. F., Ruiz-Sandoval, M. E. and Krata, N. (2004), "Smart sensing technology: opportunities and challenges", *J. Struct. Control Health Monit.*, **11**, 349-368.

Vandiver, J. K. (1975), "Detection of structural failure on fixed platforms by measurement of dynamic response", *Proc. of the 7th Annual Offshore Technology Conf.*, pp. 243-252.

Yao, G. C., Chang, K. C. and Lee, G. C. (1992), "Damage diagnosis of steel frames using vibrational signature analysis", *J. Eng. Mech.*, **118**(9), 1946-1961.

CC